



## Original Research Paper

# Wood combustion nanoparticles emitted by conventional and advanced technology cordwood boilers, and their interactions *in vitro* with human lung epithelial monolayers

Barbara Panessa-Warren<sup>1</sup>, Thomas Butcher<sup>2</sup>, John B. Warren<sup>1,\*</sup>, Rebecca Trojanowski<sup>2</sup>, Kim Kisslinger<sup>3</sup>, George Wei<sup>2</sup>, Yusuf Celebi<sup>2</sup>

<sup>1</sup>Instrumentation Division, Brookhaven National Laboratory, Upton, NY, USA.

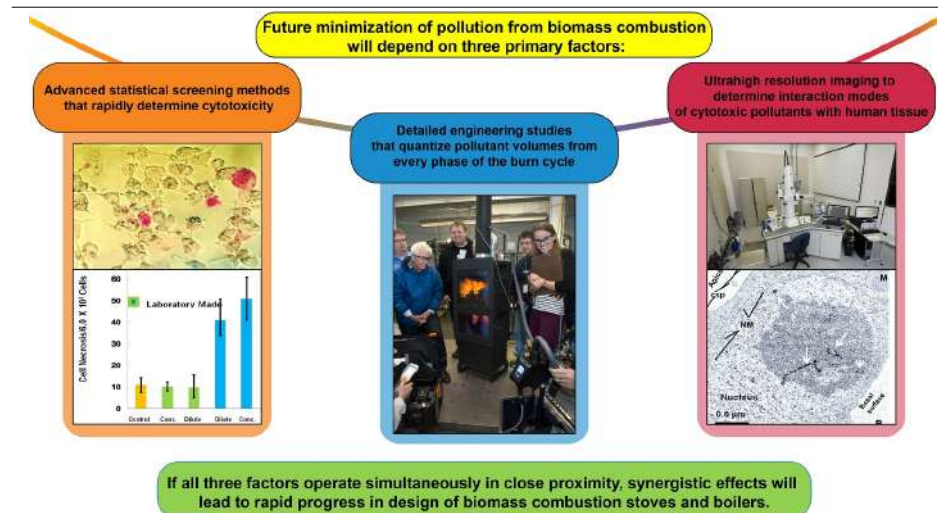
<sup>2</sup>Interdisciplinary Science Department, Brookhaven National Laboratory, Upton, NY, USA.

<sup>3</sup>Center for Functional Nanomaterials, Brookhaven National Laboratory, Upton, NY, USA.

## HIGHLIGHTS

- The morphology of combustion-emitted and lab-synthesized nanoparticles (NPs) was compared with electron microscopy.
- The composition of combustion NPs from conventional and advanced wood boilers was determined by energy dispersive X-ray analysis.
- Cell toxicity from combustion NPs (0.1 to 3.0 × 10<sup>-6</sup> kg/L aqueous solutions) was determined with optical histochemistry.
- Cytotoxicity in human lung cells was 3.5 times greater for combustion emitted NPs compared to pure graphene-based NPs.
- The mechanism of ultrastructural damage from cell-ingested NPs was studied with electron microscopy.

## GRAPHICAL ABSTRACT



## ARTICLE INFO

### Article history:

Received 28 July 2022

Received in revised form 15 August 2022

Accepted 16 August 2022

Published 1 September 2022

### Keywords:

Boiler  
Biomass combustion  
Ultrafine particle emission  
Graphene  
Cytotoxicity  
Histochemistry

## ABSTRACT

Biomass-burning boilers and stoves are widely used in many parts of the world, producing combustion emissions linked with health risks. Combustion emission nanoparticles (NPs) were collected from four representative wood burning boilers using oak cordwood at specific times in the burn cycle. The morphology and composition of the NPs was characterized using transmission electron microscopy and energy dispersive X-ray analysis. To determine the degree of NP cytotoxicity with human lung tissue, the combustion NPs were introduced to incubated lung bronchial epithelial monolayers (NCI-H292) *in vitro* at doses of 0.1 × 10<sup>-6</sup> and 3.0 × 10<sup>-6</sup> kg/L for 2 and 4 h. Histochemical analysis showed that cell death increased by a factor of 3.5 for both doses after 4 h when compared to the control. Ultrapure NPs prepared by wet chemical methods were also introduced to the epithelial lung cells for similar doses and exposure times and the cultures exhibited significantly reduced mortality. Electron microscopy was used to study the mechanism of cell mortality for the synthesized and combustion-based NPs by examining how the NP byproducts interacted with individual cell organelles. It was found that cell survival was strongly correlated with the absence of contaminants (salts, heavy metals, poly aromatic hydrocarbons) associated with the NPs entering the cells. Synthesized NPs consisting of pure carbon were relatively well tolerated and could be excreted without damaging the cell ultrastructure. Thus, careful removal of extraneous contaminants by controlling the burn cycle with a catalyst is essential to minimize the health and environmental effects of wood biofuel combustion. In better words, optimized advanced technology wood-burning boilers and stoves can provide a CO<sub>2</sub>-neutral energy source and significantly contribute to a future where fossil fuels have a reduced role.

©2022 BRTeam CC BY 4.0

\* Corresponding author at: Tel.: +1-631-682-3076  
E-mail address: [johnwarren1000@gmail.com](mailto:johnwarren1000@gmail.com)

## Contents

1. Introduction.....	1660
2. Materials and Methods.....	1661
2.1. NP collection directly on to the transmission electron microscopy EM substrate grids.....	1661
2.2. NP Collection with a thermal precipitator.....	1662
2.3. Analysis of human lung cell monolayer in vitro exposure to gas stream harvested NPs.....	1663
2.4. Lab-synthesized ultraclean NPs.....	1663
2.5. Analysis of human lung cell monolayer in vitro exposures to lab-synthesized NPs.....	1663
3. Results and Discussion.....	1664
3.1. NP characterization: outdoor conventional Boiler #1.....	1664
3.2. NP characterization: outdoor conventional Boiler #2.....	1664
3.3. NP characterization: advanced technology indoor cordwood Boiler #3.....	1664
3.4. NP characterization: advanced technology indoor Boiler #4.....	1665
3.5. Major differences between NPs generated from the four cordwood boilers.....	1665
3.6. Combustion NP interactions with human epithelial monolayers and the effect on cell mortality.....	1666
3.7. HRTEM of combustion NP interactions with cell ultrastructure.....	1667
3.8. Synthesized NP interactions with human epithelial monolayers and the effect on cell mortality.....	1668
3.9. HRTEM of synthesized NP interactions with cell ultrastructure.....	1669
4. Conclusions and Prospects.....	1669
Acknowledgements.....	1670
References.....	1670

## Abbreviations

EDX	Energy dispersive X-ray spectrometry
HRSEM	High resolution scanning electron microscopy
HRTEM	High resolution transmission electron microscopy
NP	Nanoparticle
NPA	Nanoparticle aggregates
SAED	Selected area electron diffraction
TEM	Transmission electron microscopy
PAH	Polycyclic aromatic hydrocarbon
PBS	Phosphate buffered saline
UFP	Ultrafine particle

## 1. Introduction

Throughout North America and Europe, wood boilers and woodstoves are often used to supplement the use of fuel oil or gas heating; or used as an exclusive CO<sub>2</sub>-neutral, readily available, renewable energy source. Recently, new advanced technology wood burning boilers that optimize heat production and storage for residential and institutional heating needs have been introduced globally to replace conventional wood heating appliances. These wood-burning stoves and boilers produce combustion emissions that, when inhaled have been linked to carcinogenic, respiratory, cardiovascular (Donaldson et al., 2005), and pulmonary health risks (Sarnat et al., 2008; Dorman and Ritz, 2014). Several studies have implicated wood combustion emission particulate matter as causative agents in respiratory, cardiovascular, liver, and kidney disease in exposed humans (Murr et al., 2004 and 2006; Murr, 2012). Emissions from wood and charcoal combustion contain poly aromatic hydrocarbons (PAHs), as well as resins that are known to be attached to ultrafine particles (UFPs) (Boman et al., 2003). When inhaled over time, these organic materials have been linked to toxic effects in animals (Zelikof et al., 2002) and humans (Orozco-Levi et al., 2006). Wood combustion particulates have additional reactive properties due to attached organic combustion by-products (PAHs, resins, and alcohols) released from the wood, which further increase the reactivity of the emissions and pose environmental risks (Boman et al., 2003).

Wood combustion emissions encompass a spectrum of nanoparticles (NPs) and nanoparticle aggregates (NPAs), varying in size, elemental composition, crystallinity, and reactivity. Kocbach et al. (2006 and 2009) described organic carbon, carbon soot, and inorganic ash emissions produced and released from wood-fired boilers, stoves, and fireplaces. The composition, size, and type of wood combustion particulate emissions not only depend on the heating appliance used (Torvela et al., 2014) but also the type of wood fuel burned, the moisture of the wood, the operation of the wood burning appliance, and more specifically, the conditions produced within the firebox, stack, and flue during

combustion/pyrolysis (Torvela et al., 2014). Therefore, it is essential to understand how wood boiler and stove combustion emission particulates affect exposed populations by characterizing NP emissions (<50 nm diameter) in terms of size, composition, and potential reactivity. Oberdorster et al. (2005) reported that wood combustion particulates caused lung inflammatory responses that were directly influenced by the shape, crystallinity, charge, surface modifications, and weathering of the inhaled particulates. Experimentally, it has been shown that nano-sized particles were more toxically reactive than micron-sized particles and that the surface area of inhaled NPs was linked to free radical formation, thereby promoting inflammatory responses due to oxidative stress (Murr, 2012).

Kocbach et al. (2006) described three classes of wood combustion particles; (1) spherical organic carbon, (2) soot-elemental carbon aggregates, and (3) inorganic ash particles, which are characteristically produced under specific combustion conditions. Low-temperature, incomplete combustion produced large amounts of organic spherical carbon particles; high-temperature complete combustion produced large amounts of inorganic ash particles consisting of alkali salts (KCl, K<sub>2</sub>SO<sub>4</sub>) and small amounts of trace elements. These materials can condense onto the surfaces of NPs, producing a highly reactive surface. At higher temperatures with incomplete combustion, soot is comprised of elemental carbon aggregates (turbostratic graphene spherules with variable amounts of organic compounds such as PAHs condensed onto the carbon surfaces (Rau, 1989; Braun, 2005; Frey et al., 2009). Hasler and Nussbaumer (1999) found that samples of flue gas from automatically operated wood furnaces contained 50-200 nm combustion NPs. Johansson et al. (2003) also reported UFP matter less than 1 µm in size from small-scale biomass-fired furnaces using pellets and wood briquettes for fuel. The formation of UFPs and NPAs (<100 nm), mainly composed of inorganic ash species comprised of zinc oxide particles (13 nm diameter), was reported by Torvela et al. (2014). These particles acted as nuclei for condensing inorganic vapors and organic material with an outer layer of alkali salts.

Many studies have attempted to determine the relative toxicity of NPs similar to those generated by the combustion to human lung tissue in a laboratory setting. Generally, these experiments use human lung epithelial cells such as the readily available A549 cell line (Jin et al., 2014), which is easily cultured as a monolayer in a petri dish and then exposed to aqueous concentrations of toxic agents with varying concentrations and times. In particular, NPs and NPAs derived from graphene are used for these cytotoxicity experiments since this is one of the primary components of combustion and is known to produce an inflammatory response in the lung and bronchial tissue. Many results to date have been statistical in nature and use optical microscopy to determine the degree of cell necrosis for a given concentration and exposure to a specific cytotoxic agent such as graphene or graphene oxide. Other studies used electron microscopy to image potentially damaging interactions between cell ultrastructure and NPs (Hays et al., 2007; Frontiñan-Rubio et al., 2022). While all of these studies

are useful, they ignore the fact that combustion is a complex process that produces many types of potentially cytotoxic nanomaterials.

In light of the above, a multi-faceted approach with three key elements: (1) histochemical statistics to determine cytotoxicity, (2) high-resolution electron microscopy to characterize NP and NPA morphology and to determine exactly how cell ultrastructure is degraded by combustion emitted NPs, and (3) study of “real-world” combustion by-products from existing commercial wood-based boilers is the primary purpose of this study and should provide new and useful information. This work uses these methods to study wood combustion NPs and NPAs released into the gas stream during the operation of two conventional outdoor boilers and two advanced technology indoor residential boilers. After collection, the NPs were introduced to incubated human lung bronchial epithelial cell monolayers (NCI-H292) *in vitro* to gather statistical information on how different combustion emission products affect cell toxicity using optical microscopy. Using high-resolution electron microscopy, the precise mechanism for the interaction of combustion emission NPs with cellular ultrastructure was determined by imaging how the NPs enter the cell, how they are excreted, and how they damage cell organelles.

To determine if the entry of pure carbon-based NPs alone into the exposed lung cell monolayers caused trauma and cell death or if it was caused by residues of wood combustion contaminants residing on the surface of the NPs, a protocol was developed to make graphene NPs, and graphitic spherule chains in the laboratory using ultra-clean graphene flakes swirled rapidly in a vortex solution of sterile phosphate buffered saline (PBS). These lab synthesized NPs were found to closely resemble the size and morphology of the wood combustion-produced NPs but were free of organic materials, resins, and PAHs. As in previous experiments with combustion-emitted NPs, high-resolution electron microscopy was used to study the interaction of the lab synthesized NPs with cellular ultrastructure by examining how the lab-synthesized NPs pass through cell membranes and ultimately damage cell organelles.

## 2. Materials and Methods

Four commercially-available cordwood boilers tested were operated under controlled conditions at Brookhaven National Laboratory with their operating parameters recorded for later analysis to determine how combustion conditions control the size, type, composition, and amount of the NPs, and how specific changes in the burn cycle can minimize the quantity of NPs released into the dilution tunnel. A brief description of the four different boilers is given in Table 1.

All of the wood boilers in this study were fueled with oak cordwood with attached bark. During combustion, conditions for temperatures in the stack, dilution tunnel, firebox, flue, intake and outflow temperatures of the boiler water, gases ( $O_2$ ,  $CO_2$ ,  $CO$ ) produced, types of NPs produced, fuel weight, were monitored and recorded during all phases of the burn cycle. As described by Trojanowski and Fthenakis (2019), the primary burn cycle phases are: start up, steady-state, slumber, and burn out. Each of the burn phases strongly affect the

composition and morphology of the NPs, NPAs, and gases produced by the cordwood boilers.

The NPs and NPAs were characterized morphologically with high resolution transmission electron microscopy (HRTEM) and high resolution scanning electron microscopy (HRSEM) and elementally, using energy dispersive X-ray analysis (EDX) and selected area electron diffraction (SAED). Collected NPs were isolated and separated into (a) graphene and graphitic spherule NPs; graphene and graphitic spherule clusters, chains, and fractal aggregates; and (b) the smallest nanosalt crystalline nanospherules which were released from deteriorating graphitic spherules during incomplete combustion towards the end of steady state, or during burnout when the oxygen levels were low and the carbon monoxide levels were high. Electron micrographs of the primary types of NPs are shown in Figure 1.

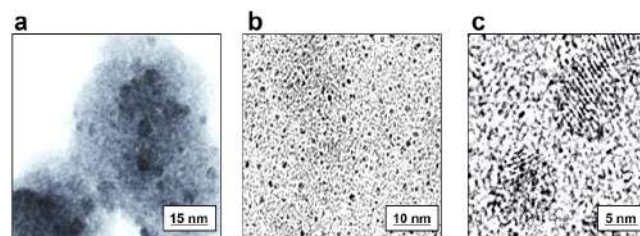


**Fig. 1.** (a) NP aggregates containing numerous electron dense spherules, (b) transmission electron microscopy (TEM) grid membrane surface covered with small electron dense dots of various shapes released from the graphitic spherules after electron beam bombardment, and (c) fully condensed nanosalt crystalline spherules (arrows), with resolved atomic lattices that appear after further electron bombardment causes localized heating. The nanosalt spherules often contain toxic metals or salts, depending on the fuel and wood burning boiler used.

### 2.1. NP collection directly on to the transmission electron microscopy EM substrate grids

NPs and NPAs were originally collected on borosilicate fiber filters positioned within the dilution tunnel of the combustion test facility at Brookhaven National Laboratory. The filters displayed a great deal of soot, organic material, and fly ash, making it difficult to isolate graphene, graphitic NP spherules and undamaged carbon spherule fractal aggregates. Removing the unwanted debris, organic matter, and larger ash from the filters, often caused damage to the smaller NPs. For high resolution morphological characterization and elemental analysis, it was necessary to obtain large amounts of ‘undamaged’ NPs that could be separated and studied individually. Then, variations in morphology and composition of the smallest crystalline spherules (1.2 to 8 nm diameter), larger graphene and graphitic spherules, and chains, fractal aggregates and clusters for various stages in the burn cycle could be categorized.

**Table 1.** Four different cordwood boilers used to study the types of wood combustion NPs released into the gas stream of the dilution tunnel during specific phases of the burn cycle. Advanced technology indoor boilers (3 and 4) and conventional outdoor boilers (1 and 2) were studied. Oak cordwood was used for all trials.

Fuel	Boilers Tested at Brookhaven National Laboratory	Boiler	Brief description of controls	Heat Output as Specified by Manufacturer (kwatt)	EPA PM 2.5 Emission Output (kg/J)	EPA PM 2.5 Emission Rate (kg/h)	Thermal Efficiency (%)
Cordwood	Indoor unit with thermal storage1- nominal 1500 liter.	3	Two-stage combustion design with oxygen and temperature sensor; 2:1 firing rate modulation ratio	20.5	$8 \times 10^{-11}$	$2 \times 10^{-3}$	69.8
		4	Induced draft with innovative nozzle design; oxygen and temperature sensors	52.7	N/A	N/A	N/A
	Outdoor unit without thermal storage	1	EPA Phase 2 Primary and secondary air damper	46.9	$13 \times 10^{-11}$	$6.4 \times 10^{-3}$	85.2
		2	EPA Phase 1 Primary air damper only	58.6	N/A	N/A	85.2



In order to collect pristine NPs from the center of the gas stream, capture devices that could be introduced into the dilution tunnel precisely when conditions were optimum (desired gas concentrations, safe temperature, desired phase of the burn cycle for sampling) were developed (Fig. 2). For the collection of HRTEM samples, a hollow metal positioning tube with a curved aluminum brace was attached to an entrance port drilled in the dilution tunnel. An insertion rod, with a copper 'clam shell clip' at the end to hold two electron microscopy grids firmly in place at the rod tip, was used to collect NPs from the center of the gas stream for each phase of the burn cycle.

The insertion rod was shielded from unwanted NP deposition by the positioning tube and then fully inserted into the gas stream at the exact time in the burn cycle and time intervals required. This avoided contaminating the grids during initial positioning, insertion, and removal. The TEM grids had a thin carbon coated membrane with patterned arrays of 2.5  $\mu\text{m}$  diameter holes, to allow debris and larger materials in the gas stream to pass through the membrane without clogging. With this device, a broad spectrum of different types of individual NPs, NPAs, and fractal agglomerates were collected for 10 to 13 min periods throughout the entire burn cycle, without the capture membranes becoming torn or covered with large fly ash, tar balls or incomplete combustion wood fibers. Following each sampling, the collection rod was kept at an ambient temperature until the TEM grid could be removed. The capture device was cleaned between sampling to prevent the build-up of combustion organic matter. To avoid corrosion damage, the collector was not used at temperatures above 310°K. This prevented NP sampling at start-up, and taking NP samples from boilers that exceeded this temperature.

## 2.2. NP Collection with a thermal precipitator

To collect larger amounts of NPs required for histochemical analysis and

cell toxicology experiments, a small thermal precipitator was inserted in the same position in the dilution tunnel as the TEM collection tube. It was designed with a  $3.0 \times 0.5$  cm flat machined on one side of a 6 mm diameter copper rod. A thin glass cover slip, coated on one side with a nichrome film, was attached to the copper flat with ceramic screws and separated by two insulating washers to form a 0.5 mm gap. The nichrome film was used as a resistor heated by a DC power supply to maintain a 100°K temperature differential between the nichrome-coated glass and the copper flat. The temperature was monitored with an Omega RDXL4SD Data Logger during collection experiments. During collection in the dilution tunnel, any NPs and NPAs that passed through the 0.5 mm gap were deposited on the nichrome-coated glass cover slip. The temperature differential was maintained by immersing the copper ribbons attached to the end of the copper rod in liquid nitrogen. With 100°K temperature differential, the collection efficiency was 99%.

The glass cover slip could then be removed from the precipitator and examined with a JEOL FE6500 field emission HRSEM. It was possible to image and elementally analyze with EDX all of the collected NPs coating the entire  $3.0 \times 0.5$  cm glass planchet without alteration. After HRSEM analysis, the NPs and NPAs were collected for cell toxicology experiments. The combined use of both types of NP collectors enabled the collection of pristine NPs and NPAs with reduced ash, organics, and debris. NPs collected on TEM grids enabled the rapid characterization of NP morphology, size, uniformity, and compositional analysis by HRTEM (using EDX, SAED, and lattice spacing measurements). NP collection with the thermal precipitator made it possible to collect large amounts of different sized NPs that could be tested for by cytotoxicity by studying their interaction with human lung epithelial monolayers.

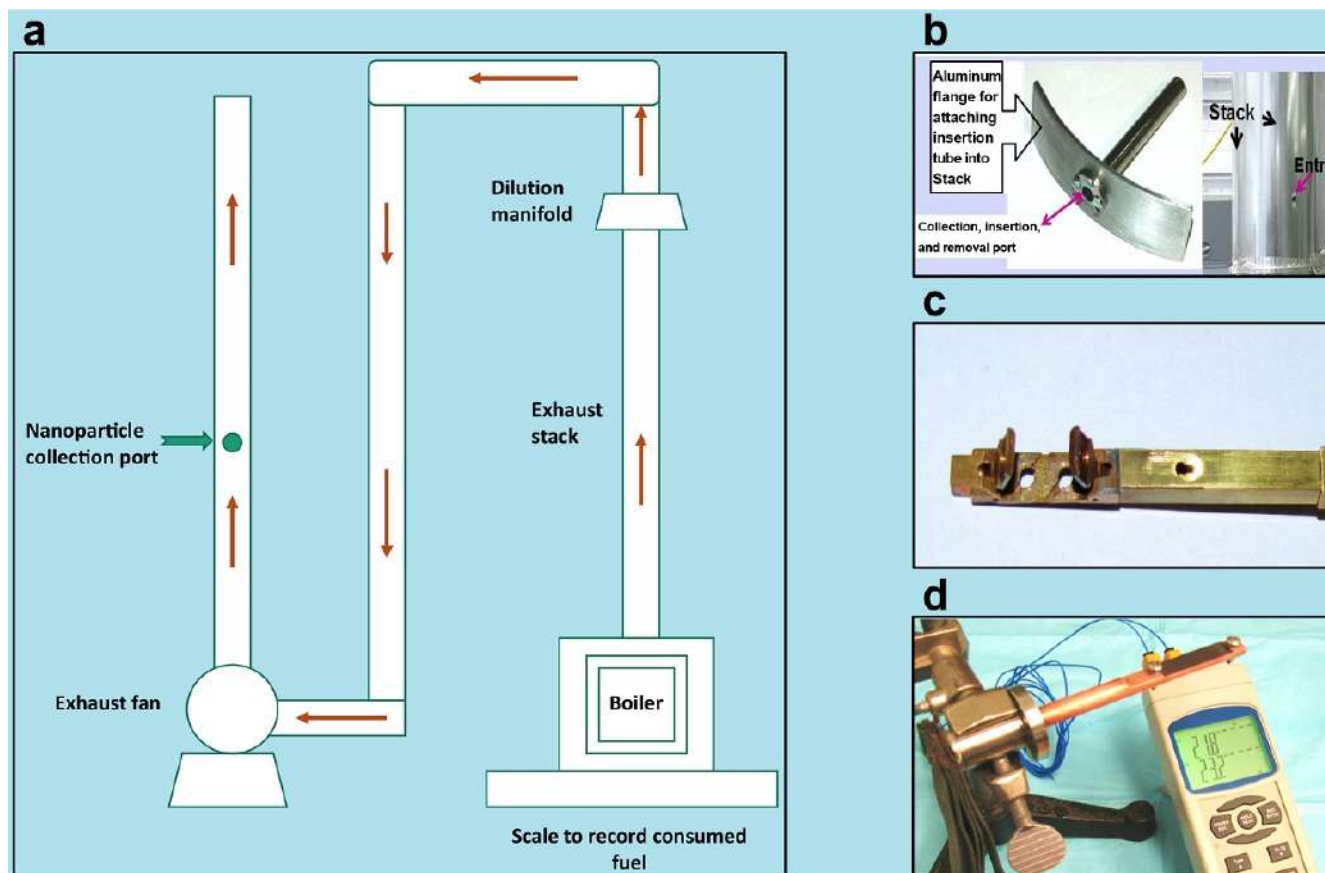


Fig. 2. (a) Schematic of boiler test facility at Brookhaven National Laboratory, showing collection port position in exhaust stack, (b and c) the insertion device and positioning tube used for NP collection in the dilution tunnel, and (d) the thermal precipitator used for large-scale NP collection.

### 2.3. Analysis of human lung cell monolayer *in vitro* exposure to gas stream harvested NPs

To understand how NPs interact with human tissue, lung cell bronchial epithelial monolayers (NCI-H292) were exposed *in vitro* to specific types of (a) characterized wood combustion graphene and graphitic spherule chains and fractal aggregates, and (b) nanosalt crystalline spherules, at high and low concentrations for 2 or 4 h exposure incubation times.

The 2 and 4 h exposures provided data about NP attachment and uptake into living lung epithelial cells, NP interactions with intracellular organelles, NP fate and excretion, signs of cellular cytotoxicity due to NP localization within cells, and NP interference with cellular function. The characterized NPs were collected from Boiler #3 because this boiler consistently produced less organic material during combustion and produced morphologically, and compositionally, characteristic graphene and graphitic spherule chains, fractal aggregates, and nano-salt crystalline nano-spherules. The boiler also operated without repeated shut-down and re-start episodes, avoiding the production of large amounts of soot and particulate matter. The collected NPs represented the classic types of wood combustion NPs released from residential chimneys into the atmosphere.

The NPs harvested from the gas stream in the dilution tunnel were isolated into two categories; (a) graphene and graphitic spherules and their nano-spherule aggregate chains, and (b) NPs consisting of nano-salt crystalline spherules. After collection, the NPs were kept in sterile, micro-centrifuge tubes in a small volume of sterile distilled water with 10% ethanol. The carbon NPs and nano-salt crystalline spherules were separated using differential micro-centrifugation. After centrifugation, the isolated graphene and graphitic spherule chains and fractal aggregates remained suspended, and were carefully removed from the vials using sterile micropipettes. The remaining liquid was further centrifuged at high speed to produce a loose pellet of nanosalt crystalline spherules. The extra supernatant was pipetted out of the centrifuge tube and the NPs were dispersed in a small volume of freshly made sterile distilled water with 10% ethanol. This process was repeated twice, and samples of the rinsed NPs were viewed with a HRSEM to ensure that no carbon NPs or their fragments had contaminated the nano-salt crystalline spherules. The isolated, cleaned NPs were kept in sterile, mini-centrifuge tubes, that were sealed and stored at 263°K until needed.

For the NP cytotoxicity experiments, human epithelial bronchial cells (NCI-H292) (Quidel Diagnostics, Athens, Ohio, USA) were grown to 95-97% confluency on 12 mm glass coverslips in individual glass vials, containing 1.5 mL of low serum (9-10%) culture medium. Monolayers exposed to NPs were incubated at 310° K for 2 or 4 h with constant rotary swirling using a Lab-line 3D Rotator to ensure the NPs dispersed evenly over the entire monolayer surface of cells. For identical exposure conditions, monolayers were grown in a low serum growth medium to which a 2  $\mu$ L dose of  $0.1 \times 10^{-6}$  kg/L of NPs (low dose) or a 2  $\mu$ L dose of  $3.0 \times 10^{-6}$  kg/L (high dose) of NPs were added. Control monolayers were given 2  $\mu$ L/mL sterile PBS added to the low serum growth medium. All of the NP exposures and controls were incubated at the same time under the same conditions with constant rotary tilting of the cells in culture medium. When working with NP interactions with human cells, the incubation medium was adjusted to contain a significantly reduced amount of serum to prevent the NPs from preferentially reacting with the human serum. This use of a low serum medium concentration insured that the NPs were free to interact with the human cells.

Following incubation, both cell monolayers exposed to NPs and the controls were rinsed with warm sterile PBS to remove unattached NPs and cellular debris, and stained with 0.4% Erythrosin B diluted 1:5 in sterile PBS (Krause et al., 1984) to count healthy and necrotic cells. After staining, the monolayers were immediately photographed using light microscopy (40 $\times$  and 200 $\times$ ), and the images digitized and enlarged for accurate cell counting of necrotic and healthy cells.

For electron microscopy, the monolayers were cleaned using the same procedure and then fixed in a 3% glutaraldehyde in 0.1 M cacodylate buffer with 0.1%  $\text{CaCl}_2$  and 7-10% sucrose, and post-fixed in 1% osmium tetroxide for 1 h. The samples were embedded in epoxy, sectioned with a microtome and examined with a JEOL1400 analytical TEM with a LaB6-gun equipped for EDX and SAED. Electron micrographs of NP attachment, entry, interactions with cellular organelles and NP excretion were taken. For higher resolution imaging, a 200KV field emission JEOL 2100 analytical HRTEM, equipped

with EDX and SAED was used. Graphene was verified by imaging and measuring the 0.34 nm lattice spacing and by SAED.

### 2.4. Lab-synthesized ultraclean NPs

To determine if the contact with the NPs was causing cell damage or elevated cell death following 4 h exposure, a technique was developed for synthesizing ultraclean, 'lab-made' graphitic NPs. These morphologically identical "lab-made" NPs were synthesized by replicating combustion conditions within a cleanroom hood. Using ultraclean graphene (Graphene Laboratories Inc., 4603 Middle Country Rd. Unit 125, Calverton, NY 11933), sterile distilled water, and sterile phosphate buffered saline to reproduce the moisture, electrolytes, and cations that were normally released from the burning cordwood, it was possible to synthesize ultraclean NPs, NPAs, graphitic fractal aggregates, and NP chains, as well as the nano-salt crystalline spherules, that were all free of any organic materials, resins or PAHs.

A non-combustion process was developed to synthesize ultra-clean graphene-based replicas of the wood combustion carbon spherule chains and fractal aggregates, based the observations seen in the early stages of wood boiler combustion. By mimicking the conditions within the wood stove firebox during start-up and early steady state, and following Schmidt et al. (2010) and Van der Wals (2007), a vortex was generated in a sterile Pyrex tube with a vortex mixer operating a 60°C. Sterile PBS provided salts that were similar to those released during oak wood combustion, and ultraclean graphene powder was sprinkled into the rotating vortex as the carbon source. The salts and electrolytes in the buffer were similar to the materials released from the oak wood burning boilers, but no heavy metals, resins, or PAHs were present. After a vortex time of 1 h, the solution was allowed to cool and settle.

Upon examination with an optical microscope at high magnification, graphene spherules and chains of spherules, and fractal aggregates were visible. The PBS solution was centrifuged and excess liquid removed. The carbon nano-spherule chains and fractal aggregates were gently pipetted into fresh small sterile vials containing double distilled water with 10% ethanol and placed in the refrigerator over-night to allow the carbon NP chains and aggregates to form a loose cloud of NPs. HRTEM and HRSEM revealed the presence of nanosalt crystalline NPs within the centers of the 'lab-made' graphitic spherules. These nanosalt crystalline spherules were partially condensed, and when imaged in the 200 KV HRTEM, the nanosalt NPs further condensed in the electron beam, forming crystalline lattices morphologically identical to the NPs and crystalline nanospherules collected from the wood combustion gas stream shown in Figure 1.

HRTEM and EDX proved the lab-made non-combustion carbon NPs and NPAs were devoid of organic PAHs, wood resins, and organic combustion products.

### 2.5. Analysis of human lung cell monolayer *in vitro* exposures to lab-synthesized NPs

The lab-made NPs described in Section 2.4 were added to human lung epithelial monolayers grown to 95-97% confluency, using the same concentrations (low dose,  $0.1 \times 10^{-6}$  kg/L and high dose,  $3.0 \times 10^{-6}$  kg/L), and exposure times (2 and 4 h) as the combustion NPs. Then responses of the human lung bronchiolar epithelial cells exposed *in vitro* to (1) collected NPs and graphitic spherule aggregates containing resins, organics, and PAHs; and to (2) to lab-made, ultra-clean graphene and graphitic spherule nano-aggregates lacking any wood combustion organic contaminants for the same time periods, at the same dose concentrations. It could then be determined if the organic materials played a major role in causing lung cell cytotoxicity or cell death; or if it was caused the entry of resin-free, PAHs-free carbon spherules, or the smallest nano-salt crystalline spherules.

As before, the cell monolayers exposed to the lab-made NPs were removed from the incubator, washed in warm buffer (to remove unattached nanoparticles and cellular waste), and prepared for light microscopy histological staining to reveal the percentage of necrotic and healthy cell populations. Samples for TEM were embedded and thin sectioned for in-depth intracellular imaging with HRTEM to study NP attachment, entry into the cell and localization within digestive vacuoles, mitochondria, nuclei, and look for evidence of intracellular NP-caused cytotoxicity.

The wood combustion collected NPs and the lab-made ultra-clean NPs used in these experiments were all initially screened and characterized by HRTEM and EDX to verify their morphology, and elemental composition checked to assure the same type of NPs was exposed to each group of cells. These *in vitro* experiments were repeated four times to insure reproducibility. The sectioned material was initially imaged unstained by HRTEM, so that the NPs within the tissue sections could be visually identified. After initial TEM imaging, the sections were stained with lead citrate and uranyl acetate and reexamined to provide clear visualization of cell membranes, organelles, and reveal signs of cytotoxicity and irreversible tissue damage.

### 3. Results and Discussion

#### 3.1. NP characterization: outdoor conventional Boiler #1

During steady state, oak cordwood combustion emission NP samples were collected from a conventional outdoor wood burning boiler (Boiler #1), and the NPs were analyzed by HRTEM, EDX, and SAED. Clusters of graphitic nano-aggregate chains comprised of oval spherules (35 to 45 nm diameter) were seen as long chains, fractal aggregates, or grouped into clusters (Fig. 3). During late steady state, the graphene began to deteriorate in the gas stream, and the nanosalt moist spherules carried within these graphitic oval capsules were able to pass out of the capsule and into the gas stream (seen on the TEM membrane as dark gray and black dots). In the gas stream, these nanosalt spherules condensed further and became smaller, eventually crystallizing and exhibiting resolved lattice planes. At high resolution, these condensing nanosalt NPs ranged in size from 1.1 to 6.0 nm diameter, and produced EDX spectra with high C and K, with slightly smaller of Na and O<sub>2</sub> peaks. This suggested that these small crystalline NPs were most likely potassium carbonate and sodium carbonate, which do not pose serious biological or environmental risks. The nanosalt crystalline spherules produced from this boiler did not display chemically or environmentally toxic crystalline salts, but they may have contained PAHs and/or resins that that could not be detected with EDX.

#### 3.2. NP characterization: outdoor conventional Boiler #2

This boiler was an outdoor, conventional updraft, staged air combustion boiler with large water, and combustion chamber volumes. This system was

refueled at multi-day intervals, and not used with external thermal storage. Air was introduced in stages inside of the single combustion chamber volume. As before, oak cordwood fuel was used during the data collection testing. During steady state, NP samples were collected from the gas stream using the thermal precipitator and imaged using HRSEM shown in Figure 4. Due to incomplete combustion, this boiler produced many different sizes of graphitic spherules. The large elliptical spherules formed clusters or small chains, which during mid-to-late steady state appeared as large capsules that were grouped together into clusters of 2-5 oval joined capsules (measuring 0.5 to 0.75  $\mu\text{m}$  in length), instead of chains and fractal aggregates. Unlike the first conventional outdoor cordwood boiler in Section 3.1, only this unit produced large graphitic capsules. Many nanosalt NPs (uncondensed spherules measuring approximately 9.0 to 22 nm in diameter), covered the thermal precipitator glass coverslip. At lower magnification, many different sizes of combustion NPs were covered with this layer of organic material. Also, a thick layer of light beige, heat sensitive, organic material covered the surface of all of the collected wood combustion NPs during late steady state. When the HRSEM electron beam was set in spot mode for EDX analysis, localized heating from the electron beam vaporized holes in the layer and removed the organic material. The longer the sample remained under the electron beam, the more this organic material was removed, revealing many smaller combustion emission NPs attached to the glass collection surface.

#### 3.3. NP characterization: advanced technology indoor cordwood Boiler #3

Boiler #3 was an indoor unit with thermal storage. It had a two-stage combustion chamber with oxygen and temperature sensors. Similar to the other boilers sampled, large graphitic spherule chains and fractal aggregates were collected containing uncondensed nano-salt spherules within graphitic capsules. The deteriorating graphitic capsule allowed nanosalt spherules (Fig. 5a, black arrows) to be deposited on the TEM membrane surface, where further condensation occurred. In this advanced technology system with a catalyst in use, small crystalline nanosalt spherules were produced that contained predominately C, Ca, O<sub>2</sub> and Na with trace amounts of Ti (Figs. 5b and c), indicating that during the final stages of condensation, toxic metals were reduced or removed by the advanced technology boiler. The Cu, Ti, P, and Si peaks in the spectra were from secondary electron

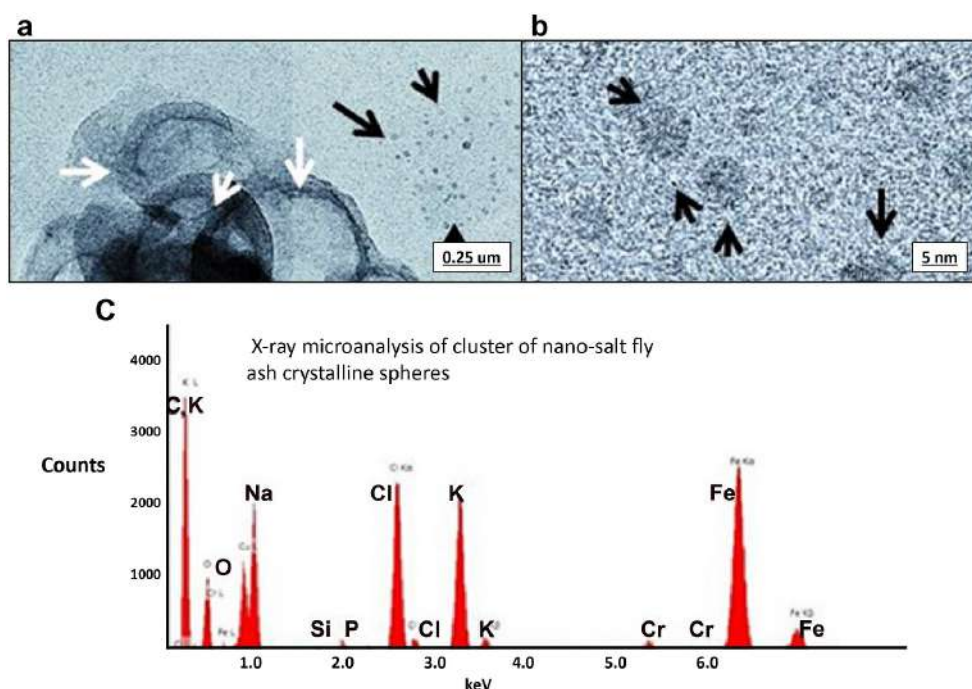


**Fig. 3.** HRTEM of NP emissions from conventional outdoor Boiler #1. Nanosalt spherules exited the graphitic capsules through deteriorating capsule walls and continued to condense in the gas stream. Isolated spherules are seen on the TEM membrane surface (a: black arrows). (b) the completely condensed nano-spherules with resolved lattice planes. (c) EDX revealing that the condensing nanosalt spherules contained C, Na, Cl, K, and O<sub>2</sub>. The Fe and Cr peaks were predominately from the sample holder.



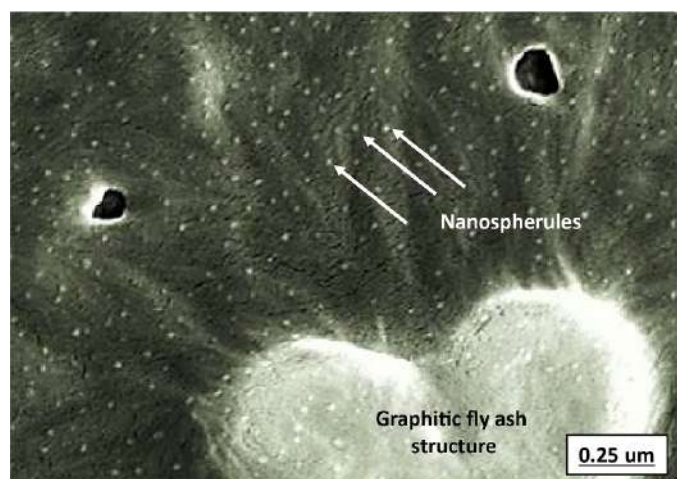


**Fig. 4.** Scanning electron micrograph of NPs from conventional Boiler #2. Similar to the Boiler #1, this system produced many large graphitic NP aggregates that were ~1 μm in size and large quantities of nanosalt spherules (white arrows). A thick organic coating covered the NPs.

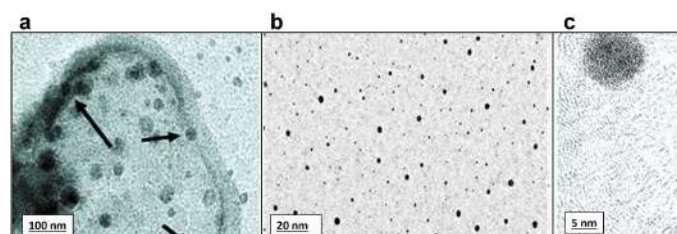


**Fig. 5.** HRTEM micrographs from Boiler #3. (a) a large graphitic capsule containing numerous nanospherules of various sizes undergoing condensation and passing out of the capsule onto the TEM membrane, (b) condensed nanosalt spherules with a size range of 1.2 to 12 nm, and (c) the smallest NPs, which are completely crystalline with resolved lattices.

scattering on to the 3.0 diameter copper TEM grid, the sample holder, and the holey membrane used to capture the NPs. This boiler exhibited reduced total emissions, and lower amounts of carbon and organic combustion material released into the gas stream. EDX spectra showed evidence of Al, Ti, Fe, Cr as well as Mg, Ca, and Si were noted when newly formed nano-salt spherules were collected, but the final analysis of the condensed nanosalt spherules and carbon NPs did not reveal high metal or carbon content. Thus, cytotoxic oxides and the presence of heavy metals were not observed during steady-state operation.

#### 3.4. NP characterization: advanced technology indoor Boiler #4

Results from advanced technology Boiler #4 were similar to Boiler #3. During steady state combustion, the collection membrane showed reduced amounts of scattered graphitic capsules (Fig. 6a). The remnants of the graphitic capsules released a halo of nanosalt uncondensed NPs. The large, darker NPs are visible as the condensation continued within the heated gas stream, the salts crystallized, producing nanosalt crystalline NPs measuring 1.2 to 9.0 nm diameter (Figs. 6b and c). SAED confirmed NP crystallization revealing soft carbon rings and well defined diffraction spots, indicating crystalline material (Fig. 6d). As these nanosalt spherules crystalized, EDX confirmed the presence of C, K, Na and O<sub>2</sub>, and lesser amounts of Cl and S suggesting predominately biodegradable salts, but no toxic metals (Fig. 6e). Like the other advanced technology boiler, only small amounts of NPs were produced. The total carbon output was low with reduced graphene and graphitic nano-aggregates. Even the smallest nanosalt NPs contained only elements that would not be considered cytotoxic, especially in these low doses.

#### 3.5. Major differences between NPs generated from the four cordwood boilers

In the previous sections, HRTEM, EDX, and SAED showed substantial differences in the morphology and composition of the NPs generated by the advanced and the conventional boilers. Conventional boilers initially produced NPs, carbon spherules and nanosalt crystalline NPs that contained some potentially cytotoxic metals (Al, Ti, Fe, Cr, Sn, and Zn). The advanced technology boilers produced NPs with predominately high K, Cl, often with Na, Ca, O<sub>2</sub>, and small amounts of P, but no heavier metals. The two advanced systems both used catalysts which seemed to be very effective in reducing both nanosalt crystalline and graphene based NP emissions. Often the TEM capture membrane in late steady state was coated with a gel-like material. Faint rings with clusters of carbon spherules trapped within the gel on the capture membrane were observed. The advanced technology boilers left nanosalt spherules with lower K, minimal or no Cl, rarely Al, but often Ca, and/or Na, and small amounts of Mg, with reduced carbon emissions left behind.

The outdoor conventional wood combustion boilers released large amounts of carbon-based NPs containing large amounts of Fe and Cr, and smaller quantities of Pb, Sn, Ti, Zn, and Al. Frequently these conventional outdoor wood boilers also produced large NPAs derived from unburned plant fibers and embedded crystals from incomplete combustion. Micron-scale tar balls and very large, dense spherules that were predominately Ca were observed during incomplete combustion. Sometimes the presence of these large, combustion aggregates tore holes in the TEM capture membranes. Although analyses of the organic combustion materials attached to the carbon and crystalline wood combustion emission particles were not attempted, the HRTEM micrographs show that the advanced technology boiler NPs had minimal organic matter attached to their surface. These NPs also did not fragment when sonicated in a 10% ethanol solution and HRSEM showed they maintained their spherical (or chain/fractal aggregate) morphologies.

Since the NPs from the advanced technology boilers were much “cleaner” than those from the conventional boilers, they were chosen for the exposure experiments with human lung bronchial epithelial cell monolayers. However, even these emission particulates varied considerably according to boiler operating conditions: how the oxygen and carbon monoxide levels are monitored and re-adjusted during operation to prevent incomplete combustion, how the temperatures in the firebox are monitored and controlled, and how the boiler design minimizes the production and release of PAHs and other organic materials that coat the surfaces of the released NPs.

The smallest combustion emission nano-salt spherules are a health risk, and in quantity can be toxic because of their (1) size (~1.2 to 8.0 nm diameter when fully condensed); (2) because the metals, or toxic salts bound within them can easily enter human cells, and (3) their crystalline structure that makes them highly reactive and capable of attachment to animal and plant cells. This crystalline nanostructure also makes them highly reactive with other NPs allowing them to combine to form large groups or islands of NPAs within individual cells. These smallest NPs can attach and pass through the cell membranes, and enter living cells, and interact with other ingested NPs to form larger structures that can damage cells by destroying intracellular organelles and/or by bioaccumulation which causes progressively more NPs to enter living cells and form islands of crystalline NPs that eventually damage intracellular organellar structures. Byrne and Baugh (2008) reported that NPs are “the most toxic component of airborne particulate matter because they have uncontrolled access to the cells of the airway and even intracellular components because of their small size”, and “that the lung exposure to nanoparticles can produce inflammatory responses due to the shape, crystallinity, charge, surface modifications and weathering of the particle”. They also noted that “many nanoparticles such as combustion derived nanoparticle agglomerates readily move as an aggregate.” Finally, a review by Trojanowski and Fthenakis (2019) note that “cleaner” advanced technology systems may produce a relatively higher percentage of NPs, even though the total particulate load decreases.

This was confirmed by HRTEM observation of the nanosalt crystalline NPs that were collected from the advanced boilers and incubated with

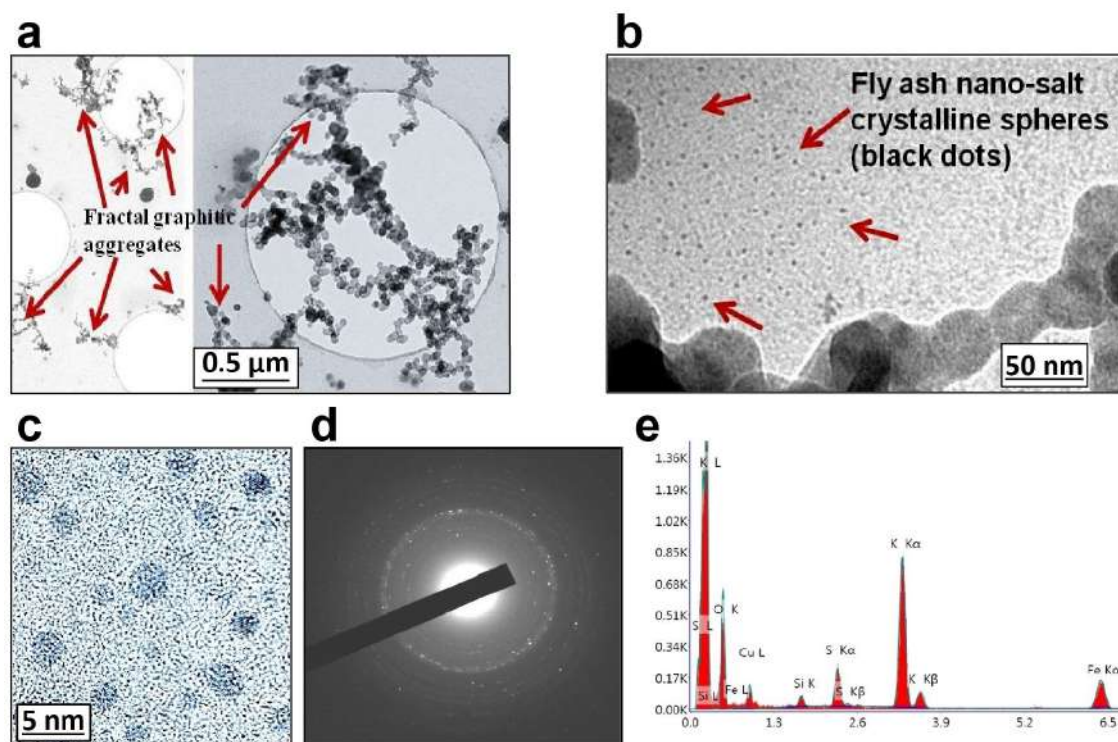


**Fig. 6.** HRTEM micrographs, SAED patterns, and EDX spectra of NP emissions from Boiler #4. (a) At low magnification and (b) at higher magnification, the remnants of the graphitic capsule (red arrows), that has released a halo of nanosalt uncondensed NPs. The large, darker NPs are the least condensed. As condensation continued within the gas stream heat, the salts crystallized, producing wood combustion nano-salt crystalline NPs (measuring ~1.2 to 8-9 nm diameter). (c) SAED confirmed NP crystallization revealing soft carbon rings with white, defined dots, indicating salt crystals. (d) As these nano-salt spherules crystallized, (e) EDX showed that they contained C, K, Na and O<sub>2</sub>, and lesser amounts of S, P and Cl.

human bronchial lung epithelium monolayers at low and high doses for 2 to 4 h (See Section 3.7). Ingram et al. (2003) showed that combustion derived NPs release transition metals or organics as their primary inflammatory mechanism leading to the production of free radicals such as superoxide anions or hydroxyl radicals and other reactive oxygen species. The HRTEM and EDX observations showed that the advanced technology boilers greatly reduced the number of NPs contaminated with metal, organic resins or PAHs that were produced by the conventional boilers.

### 3.6. Combustion NP interactions with human epithelial monolayers and the effect on cell mortality

To examine how NPs, NPAs, and the smallest nanosalt crystalline spherules interacted with living human cells, carbon spherule chains and aggregates, and nanosalt crystalline nano-spherules were isolated from an advanced technology residential wood boiler (with an operating catalyst, to provide cleaner nanoparticles with reduced organic contaminants). The NPs were cleaned in double distilled deionized water with 10% ethanol and then incubated with human (NCI-H292) lung bronchial epithelial cell monolayers grown to 95-97% confluency. The lung epithelial monolayers were exposed for 2 and 4 h, removed from the incubator, and rinsed with warm buffer to remove unattached NPs and cellular debris. Monolayers that were not exposed to NPs were prepared and used as controls. Both NP-exposed and control monolayers were then prepared for light microscopy viability staining to count necrotic and viable cells. As noted by Sato et al., (2020), most common cell lines used in these studies are derived from lung cancer cells and long-term studies of cytotoxicity should be regarded with caution. However, the 2 and 4-h exposure times used in this study are brief enough that cell degradation due to factors other than NP exposure should not affect results.

Both the NP-exposed and control monolayers were rinsed in warm buffer and prepared for thin section HRTEM imaging to examine NP attachment, entry, intracellular interactions, excretion of NPs, and identify any evidence of cellular cytotoxicity. These protocols for testing and imaging NP uptake, intracellular interactions, cellular necrosis, and NP excretion from the cells

were developed from previous studies, with various types of NPs (Panessa-Warren et al., 2008, 2009, 2012).

As described in Section 2.4, the lung cell monolayers were exposed to low ( $0.1 \times 10^{-6}$  kg/L) or high ( $3.0 \times 10^{-6}$  μg/mL) concentrations of characterized graphene and graphitic spherule chains; or nano-salt crystalline spherules, for 2 or 4 h with constant rotary mixing of the NPs within the culture media during the exposure incubation. Following incubation, the growth media was removed from the lung cell monolayers, and they were rinsed in warm buffer followed by immediate staining with Erythrosin B and photographed for statistical counting to identify necrotic and normal cells.

Matching cell monolayers incubated with the same protocol were also prepared for electron microscopy, and the sections examined unstained by HRTEM to identify where nanoparticles were found on or within cells, record how NPs entered cells, and identify any signs of cellular cytotoxicity or other pathology. These TEM sections were then stained to reveal organellar membranes and screen for signs of cytotoxicity, NP-degradation, excretion by the cell, or cell death. These experiments were repeated four times using NCI-H292 cell monolayers, to determine if the results were consistent for each group of samples.

After a 2 h exposure, the results showed that regardless of the concentration of the wood combustion graphene spherule chains and fractal aggregates, the lung cells showed the same mortality rate, which was approximately 3 times greater than control values (Fig. 7). However, the cell monolayers exposed to the lower dose of wood combustion nanosalt spherules for 2 h showed only a small increase in cell mortality. At the higher dose of wood combustion nanosalt spherules cell death was almost 3.5 times greater than the lower dose. For the 4 h exposure, there was no statistical difference between the cell death rate caused by the graphene spherules or the nanosalt spherules at low and high dose exposure incubations. Only the low dose of the nanosalt spherules at 2 h was closer to the control level, suggesting that for the shorter time period, the lung cells may have been able to cope with this volume of foreign material with



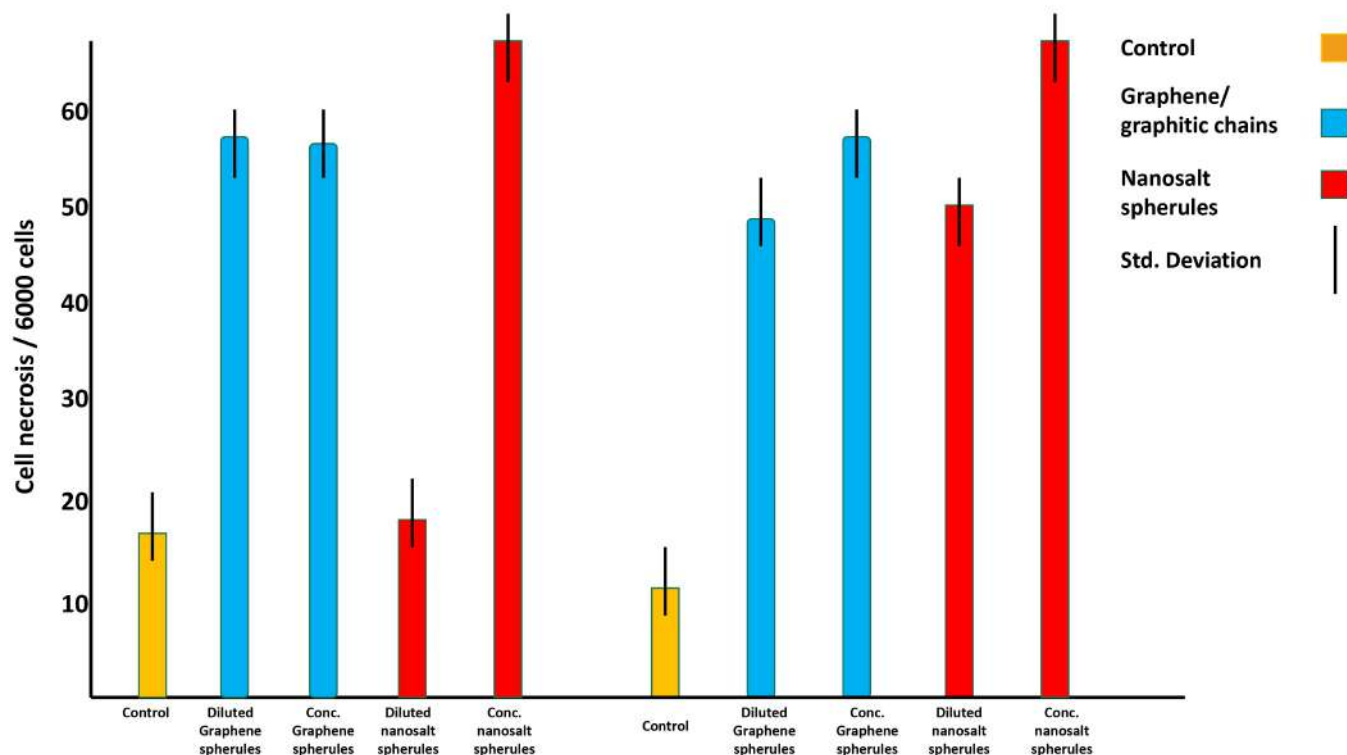


Fig. 7. Comparison of human lung bronchiolar epithelial cell monolayers exposed to  $0.1 \times 10^{-6}$  kg/L and  $3.0 \times 10^{-6}$  kg/L aqueous solutions of wood combustion NP aggregates and nanosalt crystalline spherules, compared to unexposed incubated cells used as a control.

only a slight increase in cell death. This latter outcome was confirmed by the HRTEM of the nanosalt spherule exposed lung cell monolayers. While the nanosalt crystalline spherules entered the lung cells, the number of internalized nanosalt crystalline spherules did not damage many of the intracellular organelles, and the cells were able to survive. However, cell death at the higher dose of nanosalt crystalline spherules clearly showed death by “bioaccumulation”. This was repeated in the nanosalt spherule low and high dose exposures of the lung epithelial cells for the 4 h exposure where the cell death was 3-4 times higher than control values.

### 3.7. HRTEM of combustion NP interactions with cell ultrastructure

HRTEM of cells exposed to  $0.1 \times 10^{-6}$  and  $3.0 \times 10^{-6}$  kg/L NP doses are shown in Figure 8. These smallest NPs with their highly reactive crystalline surface were able to pass through the human apical cell membranes via the lipid regions. Consequently, the cells were not able to control uptake of the nanosalt crystalline NPs by endocytosis or any cell mediated process. Because of their reactivity, these smallest NPs will readily combine to form NP clusters within the human cell's cytoplasm, and the clusters will continue to grow during the incubation process. For low doses ( $0.1 \times 10^{-6}$  kg/L), this aggregation process was retarded due to the increased distances between the initial NPs that had penetrated the cell. However, at a 2 h incubation with the higher dose of nanosalt spherules ( $3.0 \times 10^{-6}$  kg/L), the cell rapidly filled with hundreds of crystalline NPs. As they joined together in clusters, their reactive borders touched and damaged intracellular organelles within the cytoplasm, rupturing membranes, and preventing the cells' ability to capture the NPs in digestive vacuoles to be chemically degraded and excreted at the basal cell surface. At the high dose ( $3.0 \times 10^{-6}$  kg/L), the cells for both the 2 and 4 h exposures became overwhelmed and no longer had intact mitochondria used for ATP energy production; no visible endoplasmic reticulum membranes and no intact Golgi organelles. Some cells were so filled with large islands of nanoparticles that it was only possible to see outlines of broken vacuolar membranes and regions of cytoplasm filled with rows of dense clusters of nanosalt crystalline NPs.

These nanosalt crystalline spherules are the smallest combustion emission NPs (1.2 - 8.0 nm), that were routinely produced from all of the wood

combustion boilers tested. Because of their small size, along with their final crystallized morphology, they are highly reactive and can easily enter living cells. These NPs have the potential to pose significant health risks if produced in large numbers. Efforts to avoid the formation and release of this type of nanosalt crystalline spherule should be directed at reducing the formation of graphitic spherule chains and fractal aggregates. This can be achieved by minimizing the time graphitic spherules spend in an environment with moisture and salts that could combine within the graphitic capsules, thereby eliminating the formation of the spherules during mid or late steady state, or burnout. The highest production of these spherules was observed prior to burnout and during periods of low oxygen and high carbon monoxide.

Advanced technology wood boilers and advanced wood stoves already have automatic monitoring of oxygen and carbon monoxide production, and the gas levels associated with incomplete combustion can be altered to reduce production of these smallest, reactive NP emissions. EDX of these large nanosalt crystalline islands often revealed Al, Mg, Ti, Si, C as well as Ca, P, Cl, Na, and O<sub>2</sub> early during steady state. However, in the advanced technology wood boilers, the composition of these smallest nanosalt spherules changed with the boiler used, with a reduction in heavy metals, producing a less reactive nanosalt NP. Although this was achieved mostly with catalyst use, changes in the operating conditions also altered NP composition prior to release, reducing environmental risk.

The graphically summarized cytotoxicity results showed increased cell deaths from cells exposed to the wood combustion produced carbon spherule NPs. This sensitivity was most likely due to organic materials (PAHs, resins) that were trapped on or within the NPs (Li et al., 2003). However, the increased mortality could also have been caused by the trauma suffered by the cells during the entry of the spherule chains into the cytoplasm causing unrepairable damage to the apical cell surface. These interactions with internal cell membranes prevented the cell from repairing these penetrations. Alternatively, the nanosalt crystalline NPs passing through the apical membrane may have started to release cytotoxic salts (oxides, hydroxides or metal salts), which denatured the internal organelles and proteins.

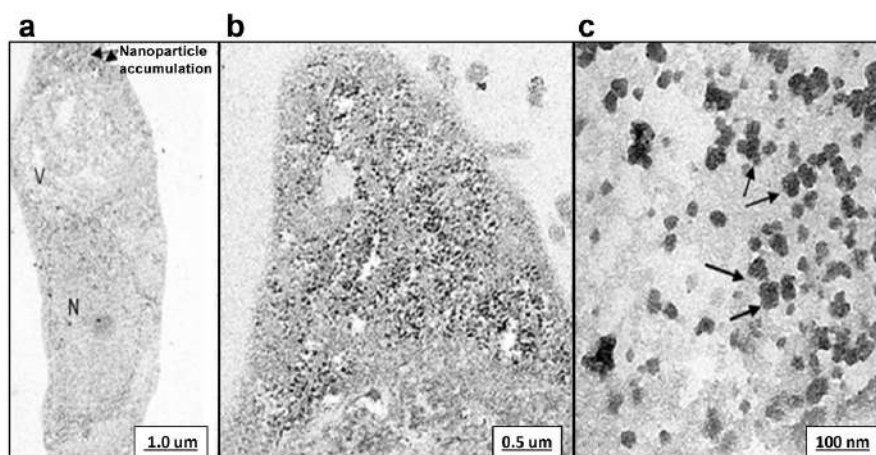


**Fig. 8.** (a) A view of an entire lung cell showing uptake of nanosalt crystalline NPs, accumulating in the cell tip, nucleus (N) and vacuoles (V). (b and c) Higher magnification views of the cell tip reveal aggregated crystalline NPs joined together to make 60-100 nm islands of nanosalt crystalline spherules, filling the cytoplasm, damaging organellar membranes, and causing the destruction of the intracellular organelles needed for cell survival.

### 3.8. Synthesized NP interactions with human epithelial monolayers and the effect on cell mortality

To determine which of two mechanisms proposed in Section 3.7 led to elevated cell mortality, the lab synthesized NPs were exposed the human bronchial epithelium cells using the same concentrations and exposure times as the combustion-based NPs. The synthesized NPs were separated into two groups; (1) graphene and graphitic spherule chains, and (2) dense accumulations of nanosalt crystalline nano-spherules. They were placed in separate sterile micro-centrifuge tubes at 373°K until needed for an experiment with the cells, or for HRTEM characterization of their composition or morphology. The smallest nanoparticles were sonicated briefly to keep them from joining into islands, and then weighed and diluted to the  $0.1 \times 10^{-6}$  kg/L and  $3.0 \times 10^{-6}$  kg/L concentrations needed for the low dose/high dose exposure experiments with the human lung epithelial monolayers, respectively. While

graphene-derived NPs and their interactions with lung tissue are mentioned frequently in the recent literature (Fadeel et al., 2018; Liao et al., 2018; Pelin et al., 2018; Tabish et al., 2018; Di Cristo et al., 2020), only a few studies actually consider both synthesized graphene NPs with ultrastructural studies *via* HRTEM. Only one recent study (Frontiñan-Rubio et al., 2022), actually used HRTEM and graphene-based materials for cyto-toxicology studies but the graphene-based NPs were not directly compared to combustion-based NPs.

As shown in Figure 9, no increase in cell necrosis compared to the control was observed following the 4 h exposure of human lung monolayers exposed to the lab-synthesized, ultra-clean graphene spherules at either the high dose or the low dose (green bars). In contrast, exposure of lung cell monolayers to the combustion-based graphene spherules produced significantly greater cell death (blue bars). The cells exposed to the lowest dose of the  $0.1 \times 10^{-6}$  kg/L wood combustion graphene spherules revealed

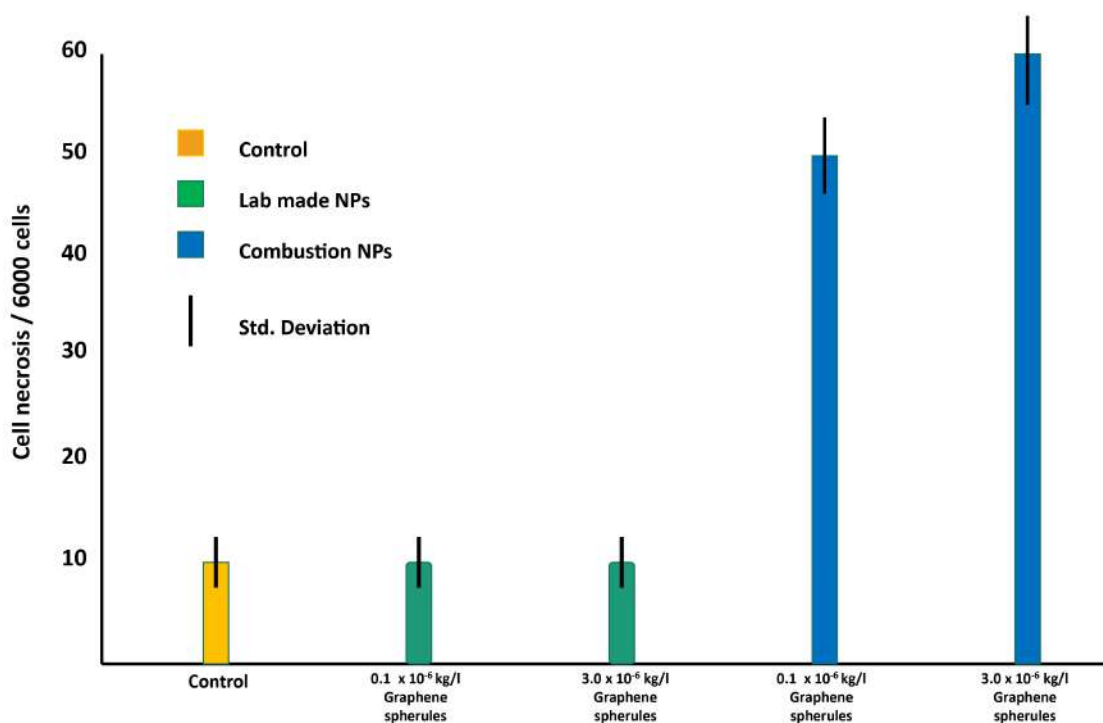


**Fig. 9.** Lung epithelial cell responses *in vitro* to ultra-clean lab-synthesized graphene and graphitic nano-spherules and compared to combustion-based equivalents.

more than a two-fold increase in cell death compared to the control level; and the cell monolayers incubated with the wood combustion graphene spherules at the higher dose ( $3.0 \times 10^{-6}$  kg/L) or 4 h revealed slightly higher numbers of dead human lung epithelial cells compared to the control. These results indicated that the lab-synthesized graphene spherules at low and high doses did not produce cell death even though these NPs are the same size as the combustion-based NPs. Therefore, the ability of NPs composed only of graphene to enter the cells did not produce cell trauma and necrosis. This must be compared to the death rate that was 3.5 times greater for combustion graphene spherules. This strongly suggests that retained material from combustion-based graphene and graphitic nanospherules caused the increased cell death, not the interaction with the carbon, or the penetration of the cells by the NPs.

### 3.9. HRTEM of synthesized NP interactions with cell ultrastructure

In these experiments, the NPs and nano-aggregates did not have any combustion resins or PAHs on or within their surfaces. When the lab-synthesized, ultra-clean carbon spherule nano-aggregates interacted with the lung cell surfaces, they became coated with mucus as they entered the apical cell membrane which may have facilitated penetration through the bronchial cell wall. These bronchial epithelial cells normally recycle mucus components. The mucus on the cell surface functions to trap particulates that are inhaled, and prevent them from going deeper into areas of the bronchial tree, thereby protecting the oxygen exchange areas of the lung.

The graphical evidence of cell mortality in Figure 9 can be compared to HRTEM of the cell ultrastructure. In Figure 10, this is shown with a micrograph of the ultraclean NPs actually entering the lung cell walls. In Figure 10a, the darker staining spherical structure within the nucleus is the nucleolus (responsible for ribosome manufacture), which contains entire chains of carbon nanospherules (white arrows) which have passed into this structure without killing the cell.

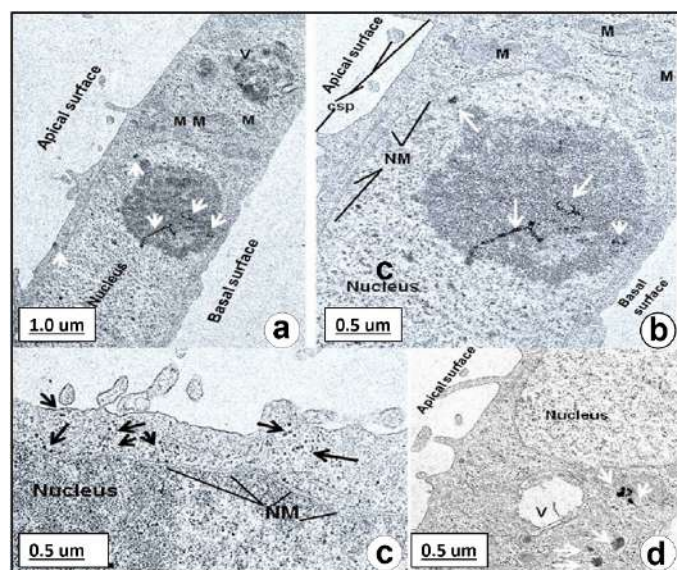


**Fig. 10.** Lab-made NPs and nano-aggregates can be seen within the lung bronchial epithelial cells, after a 4 h incubation. Clusters of nanoparticles shown by the white arrows can be seen in the cytoplasm (white arrows), and within the nucleus. (a and b) rapid entry of the NPs into the lung cells directly through the apical membrane and passage into the cytoplasm, nucleus, and nucleoli (central white arrows); (b and c) cytoskeletal projections and entry of NPs (black arrows) into cytoplasm; (d) digestive vacuole (V) and excretion vacuoles with black digested carbon NPs to be excreted at the basal membrane surface.

A vacuole (V) containing digested carbon and some NPs and debris which is being taken to the basal cell surface for excretion. At higher magnification (Fig. 10b), the lab-made graphene aggregates were seen intact within the nucleus and nucleolus (white arrows) without any apparent damage to the cell

membranes. The nuclear membrane was still intact with normal mitochondria and endoplasmic reticulum visible, and small clumps of carbon inclusions visible within the nucleus. In Figure 10c, many carbon spherules were seen within the cytoplasm, passing through the apical cell surface and within the nucleus and nucleolus (black arrows) and passing through the nuclear membrane (NM). After 4 h, some cells were able to digest the carbon material (Fig. 10d) and release the globular digested carbon into vacuoles (white arrows) for excretion at the basal membrane. These results correspond with the statistical findings for the 4 h exposures of lung cell monolayers where there was no cell death with the synthesized ultraclean nanoparticles.

## 4. Conclusions and Prospects

This work attempts to characterize NPs generated from both conventional and advanced technology oak wood fueled boilers. The NPs were collected from the gas stream and deposited directly onto 3.0 mm grids used for TEM examination or onto flat substrates *via* thermal precipitation. Samples deposited on TEM grids were characterized with HRTEM, EDX, and SAED. Samples deposited on glass substrates were collected and introduced to cultured human epithelial cells to determine cell toxicity. In addition, a method was developed to synthesize ultrapure NPs from a graphene precursor *via* a non-combustion-based process. These NPs were also introduced to the human epithelial cell cultures to act as a control.

HRTEM showed that the NPs collected from all 4 boilers displayed a variety of morphologies ranging from isolated NPs 2 to 4 nm in diameter to NP agglomerates and chained graphitic spherules that were 10s of nm in length. EDX spectra showed these carbon-based contained heavy metal ions, particularly those from the conventional boilers. Common to emissions from all 4 boilers, all were small nanoscale crystalline NPs with resolved lattice planes. HRTEM of the synthesized NPs showed the same types of particles as the combustion NPs, but no heavy metal, PAH, or resinous film contamination.

When the combustion-based NP solutions were added to incubated cells layers in a low dose ( $0.1 \times 10^{-6}$  kg/L) and a high dose ( $3.0 \times 10^{-6}$  kg/L) for 2 and 4 h, it was found that cell mortality increased by a factor of 3.5 for both doses and exposure times. Graphical evidence could not distinguish whether cell mortality increased strictly from large numbers of spherules contaminated by PAHs and heavy metals being ingested by the cells or by bioaccumulation where large numbers of small nanoscale NPs combined together after cell entry and destroyed cell functionality simply by their large numbers.

When this experiment was repeated for the synthesized NP solutions with the 4 h exposure time, no increase at all in cell mortality was seen for both the  $0.1 \times 10^{-6}$  kg/L and  $3.0 \times 10^{-6}$  kg/L concentrations. Since the synthesized NP solution contained both nanoscale NPs formed from the saline buffer solution and large graphene spherules, it is apparent that the cells could tolerate relatively large amounts of graphene-derived and alkali salt NPs as long they were not contaminated with materials typically found in combustion products from conventional wood boilers.

These experiments showed that the interactions of these predominately graphene and graphitic spherule chains and fractal aggregates do not cause cell death or damage to the lung epithelial cells even when these long chains of carbon spherules travel into a cell membrane, through the cytoplasm and pass directly into the cell's nucleus. Sometimes, entire fractal aggregate chains of carbon nanospherules within a cell's nucleus were observed and the cell did not die nor showed signs of cytotoxicity. However, when cells were exposed to graphene and graphitic spherule chains from the wood combustion boilers, the cells experienced almost a 3.5-fold increase in cell death compared to control values after 4 h exposure periods. It was clear from these results that there was something additional on, or within, the NPs produced in the wood combustion boilers that increased cell toxicity.

It is postulated that the graphene spherule chains and graphitic spherule fractal aggregates from wood combustion boilers acts as a "Trojan Horse" covered with organic material (resins, PAHs) that coat or contaminate the surface of the NPs. Alternatively, these contaminants can be embedded internally the spherule chains or clusters. Thus, the carbon spherules and fly ash serve as vehicles to carry combustion chemicals into the atmosphere and disseminate them, posing health risks to humans and the environment in general.



In conclusion, the conventional and advanced technology cordwood-burning boilers all produced the same types of NPs (graphene spheres, graphitic spheres containing condensing salt nano-spherules and various forms of fly ash). However, the advanced technology boilers using catalysts showed significant reductions of both graphene spherule chains, and graphitic chains containing nanosalt spherules with an assortment of potentially toxic metals such as Al, Ti, Cr, Fe, Mg, and Mn. Optimum operating conditions also contribute to the generation of fewer NPs, with low atomic number composition for those that do occur. Human lung cell exposure experiments revealed that combustion-based graphene and graphitic NP chains passed into cells and caused a two-fold increase in cell death; as did also the smallest crystalline nano-salt spherules. However, when clean graphene and graphitic structures containing sterile salt nanospheres were exposed to human cells, mortality did not increase above control values. This suggests that human lung cells do not show toxicity following short term contact with clean graphene and graphitic spheres of this size. It therefore seems that contaminants generated by combustion bind to these carbon NPs and these contaminants are responsible for the observed cell necrosis, even at low doses. Cordwood which does not contain tree bark minimizes the risk of the release of heavy metals, organics, PAHs, oils, terpenes, and other chemicals linked to human health risks and environmental contamination.

The results from this research show that design of advanced combustion systems that burn off combustion materials while using catalysts to capture specific toxic materials and optimize burning parameters to produce less reactive emissions will be of critical importance to minimize health and environmental effects. Optimized advanced technology wood-burning boilers and stoves can provide a CO<sub>2</sub>-neutral energy source and significantly contribute to a future where fossil fuels have a reduced role.

#### Acknowledgements

The authors would like to acknowledge the New York State Energy and Research Development Authority that funded this project (Project number 29697, and Agreement number 63038), and provided an environment to meet many experts in the field of biomass combustion engineering research, manufacturers, and designers of new and innovative boiler & wood stove designs, and learn about wood combustion health effects, in an environment of creative collaboration. We would also like to thank Dr. Ellen Burkhard of NYSEDA who facilitated the development and completion of this project. This research was carried out (in part) at the Center for Functional Nanomaterials at Brookhaven National Laboratory, supported by the US Department of Energy, Office of Basic Energy Sciences, under Contract No. DE-ACO2-98CH10886.

#### References

- [1] Boman, B.C., Forsberg, A.B., Järnholm, B.G., 2003. Adverse health effects in relation to residential wood combustion in modern society. *Scand. J. Work Environ. Health*. 29(4), 251-260.
- [2] Braun, A., 2005. Carbon speciation in airborne particulate matter with C (1s) NEXAFS spectroscopy. *J. Environ. Monit.* 7(11), 1059-1065.
- [3] Byrne, J.D., Baugh, J.A., 2008. The significance of nanoparticles in particle induced pulmonary fibrosis. *McGill J. Med.* 11(1), 43-50.
- [4] Di Cristo, L., Grimaldia, B., Catelani, T., Vazquez, J.E., Ampofo, P.P., Sabella, S., 2020. Repeated exposure to aerosolized graphene oxide mediates autophagy inhibition and inflammation in a three-dimensional human airway model. *Mater. Today Bio.* 6, 100050.
- [5] Donaldson, K., Tran, L., Jimenez, L.A., Duffin, R., Newby, D.E., Mills, N., MacNee, W., Stone, V., 2005. Combustion-derived nanoparticles: a review of their toxicology following inhalation exposure. *Part. Fibre Toxicol.* 2(1), 10.
- [6] Dorman, S.C., Ritz, S.A., 2014. Smoke exposure has transient pulmonary and systemic effects in wildland firefighters. *J. Respir. Med.* 2014, 1-9.
- [7] Fadeel, B., Bussey, C., Merino, S., Vázquez, E., Flahaut, E., Mouchet, F., Evariste, L., Gauthier, L., Koivisto, A.J., Vogel, U., Martín, C., Delogu, L.G., Buerki-Thurnherr, T., Wick, P., Beloin-Saint-Pierre, D., Hischer, R., Pelin, M., Carniel, F.C., Tretiac, M., Cesca, F., Benfenati, F., Scaini, D., Ballerini, L., Kostarelos, K., Prato, M., Bianco, A., 2018. Safety assessment of graphene-based materials: focus on human health and the environment. *ACS Nano*. 12(11), 10582-10620.
- [8] Frey, A.K., Tissari, J., Saarnio, K.M., Timonen, H.J., Tolonen-Kivimäki, O., Aurela, M.A., Saarikoski, S.K., Makkonen, U., Hytönen, K., Jokiniemi, J., Salonen, R.O., Hillamo, R.E.J., 2009. Chemical composition and mass size distribution of fine particulate matter emitted by a small masonry heater. *Boreal Environ. Res.* 14, 255-271.
- [9] Frontiñan-Rubio, J., González, V.J., Vázquez, E., Duran-Prado, M., 2022. Rapid and efficient testing of the toxicity of graphene-related materials in primary human lung cells. *Sci. Rep.* 12(1), 7664.
- [10] Hasler, P., Nussbaumer, T., 1999. Gas cleaning for IC engine applications from fixed bed biomass gasification. *J. Biomass Bioenergy*. 16(6), 385-395.
- [11] Hays, M.D., Vander Wal, R.L., 2007. Heterogeneous soot nanostructure in atmospheric and combustion source aerosols. *Energy Fuels*. 21(2), 801-881.
- [12] Ingram, J., Rice, A., Santos, J., Van Houten, B., Bonner, J.C., 2003. Vanadium-induced HB-EGF expression in human lung fibroblasts is oxidant dependent and requires MAP kinases. *Am. J. Physiol. Lung Cell. Mol. Physiol.* 284(5), L774-L782.
- [13] Jin, C., Wang, F., Tang, Y., Zhang, X., Wang, J., Yang, Y., 2014. Distribution of graphene oxide and TiO<sub>2</sub>-graphene oxide composite in A549 cells. *Biol. Trace Elem. Res.* 159(1-3), 393-398.
- [14] Johansson, L.S., Tullin, C., Leckner, B., Sjövall, P., 2003. Particle emissions from biomass combustion in small combustors. *Biomass Bioenergy*. 25(4), 435-446.
- [15] Krause, A.W., Carley, W.W., Webb, W.W., 1984. Fluorescent erythrosin B is preferable to Trypan Blue as a vital exclusion dye for mammalian cells in monolayer culture. *J. Histochem. Cytochem.* 32(10), 1084-1090.
- [16] Kocbach, A., Li, Y., Yttri, K.E., Cassee, F.R., Schwarze, P.E., Namork, E., 2006. Physicochemical characterization of combustion particles from vehicle exhaust and residential wood smoke. *Part. Fibre Toxicol.* 3(1), 1-10.
- [17] Kocbach Bølling, A., Pagels, J., Yttri, K.E., Barregard, L., Sallsten, G., Schwarze, P.E., Boman, C., 2009. Health effects of residential wood smoke particles: the importance of combustion conditions and physicochemical particle properties. *Part. Fibre Toxicol.* 6(1), 29.
- [18] Liao, Y., Wang, W., Huang, X., Sun, Y., Tian, S., Cai, P., 2018. Reduced graphene oxide triggered epithelial-mesenchymal transition in A549 cells. *Sci. Rep.* 8(1), 15188.
- [19] Li, N., Sioutas, C., Cho, A., Schmitz, D., Misra, C., Sempf, J., Wang, M., Oberley, T., Froines, J., Nel, A., 2003. Ultrafine particulate pollutants induce oxidative stress and mitochondrial damage. *Environ. Health Perspect.* 111(4), 455-460.
- [20] Murr, L.E., Esquivel, E.V., Bang, J.J., 2004. Characterization of nanostructure phenomena in airborne particulate aggregates and their potential for respiratory health effects. *J. Mater. Sci. Mater. Med.* 15(3), 237-247.
- [21] Murr, L.E., Soto, K.F., Garza, K.M., Guerrero, P.A., Martinez, F., Esquivel, E.V., Ramirez, D.A., Shi, Y., Bang, J.J., Venzor III, J., 2006. Combustion-generated nanoparticles in the El Paso, TX, USA/Juarez, Mexico Metroplex: their characterization and potential for adverse health effects. *Int. J. Environ. Res. Public Health*. 3(1), 48-66.
- [22] Murr L. 2012. Chapter 1: soot: structure, composition, and health effects: Paul, M.C. (Ed.), soot: sources, formation and health effects. Nova Science, New York.
- [23] Oberdorster, G., Oberdorster, E., Oberdorster, J., 2005. Nanotoxicology: an emerging discipline evolving from studies of ultrafine particles. *Environ. Health Perspect.* 113(7), 823-839.
- [24] Orozco-Levi, M., Garcia-Aymerich, J., Villar, J., Ramirez-Sarmiento, A., Anto, J.M., Gea, J., 2006. Wood smoke exposure and risk of chronic obstructive pulmonary disease. *Eur. Respir. J.*, 27(3), 542-546.
- [25] Rau, J.A., 1989. Composition and size distribution of residential wood smoke particles. *Aerosol Sci. Technol.* 10(1), 181-192.
- [26] Sarnat, J.A., Marmur, A., Klein, M., Kim, E., Russell, A.G., Sarnat, S.E., Mulholland, J.A., Hopke, P.K., Tolbert, P.E., 2008. Fine particle sources and cardiorespiratory morbidity: an application of chemical

- mass balance and factor analytical source-apportionment methods. *Environ Health Perspect.* 116(4), 459-466.
- [27] Panessa-Warren, B.J., Warren, J.B., Maye, M.M., Van Der Lelie, D., Gang, O., Wong, S., Ghebrehwet, B., Tortora, G., Misewich, J., 2008. Human epithelial cell processing of carbon and gold nanoparticles. *Int. J. Nanotechnol.* 5(1), 55-91.
- [28] Panessa-Warren, B.J., Maye, M.M., Warren, J.B., Crosson, K.M., 2009. Single walled carbon nanotube reactivity and cytotoxicity following extended aqueous exposure. *Environ. Pollution.* 157(4), 1140-1151.
- [29] Panessa-Warren, B., Warren, J., Kisslinger, K., Crosson, K., Maye, M.M., 2012. Human airway epithelial cell responses to single walled carbon nanotube exposure: nanorope-residual body formation. *Nanosci. Nanotechnol. Lett.* 4(11), 1110-1121.
- [30] Pelin, M., Sosa, S., Prato, M., Tubaro, A. 2018. Occupational exposure to graphene-based nanomaterials: risk assessment. *Nanoscale.* 10(34), 15894-15903.
- [31] Sato, M., Shay, J.W., Minna, J.D., 2020. Immortalized normal human lung epithelial cell models for studying lung cancer biology. *Respir. Invest.* 58(5), 344-354.
- [32] Tabish, T.A., Pranjal, M.Z.I., Hayat, H., Rahat, A.A., Abdullah, T.M., Whatmore, J.L., Zhang, S., 2017. *In vitro* toxic effects of reduced graphene oxide nanosheets on lung cancer cells. *Nanotechnol.* 28(50), 504001.
- [33] Torvela, T., Tissari, J., Sippula, O., Kaivosoja, T., Leskinen, J., Virén, A., Lähde, A., Jokiniemi, J., 2014. Effect of wood combustion conditions on the morphology of freshly emitted fine particles. *Atmos. Environ.* 87, 65-76.
- [34] Trojanowski, R., Fthenakis, V., 2019. Nanoparticle emissions from residential wood combustion: a critical literature review, characterization, and recommendations. *Renew. Sust. Energy Rev.* 103, 515-528.
- [35] Zelikoff, J.T., Chen, L.C., Cohen, M.D., Schlesinger, R.B., 2002. The toxicology of inhaled wood smoke. *J. Toxicol. Environ. Health Part B.* 5(3), 269-282.



**Barbara Panessa-Warren** is a cell biologist who earned her PhD from New York University. She served as a professor at Stony Brook University and as a research scientist at Brookhaven National Laboratory. She has many years of experience as an electron microscopist with a research focus on the effects of nanomaterials on biological tissue.



**John Warren** served as a research scientist in the Instrumentation Division of Brookhaven National Laboratory for over 40 years. He earned his PhD in Materials Science at the University of Florida. At Brookhaven, he has specialized in micro and nano fabrication technology and was responsible for the design of the Nanofabrication Facility at the Center for Functional Nanomaterials at Brookhaven.



**Thomas Butcher** is a Research Engineer and Head of the Energy Conversion Group at Brookhaven National Laboratory. He earned his PhD in Mechanical Engineering at Stony Brook University and also studied at Stevens Institute and the U.S. Merchant Marine Academy. Dr. Butcher has many years of experience in research at BNL related to building energy systems, the combustion of novel biofuels, and emissions measurements.



**Rebecca Trojanowski** is an engineer within the Energy Conversion group at Brookhaven National Laboratory. Her interests focus on research and development efforts to advance building energy systems, reduce fossil fuel dependency, and technical solutions to reduce combustion related emissions. She has focused much of her career on biomass combustion and the related emissions after graduating from Worcester Polytechnic Institute and while continuing to pursue her PhD at Columbia University.



**Kim Kisslinger** is a technical staff member in the Center for Functional Nanomaterials (CFN) at Brookhaven National Laboratory. Kim has over 12 years of experience in the semiconductor industry (most recently with Intel Corp) as a transmission electron microscopy associate producing TEM samples and performing TEM/STEM/SEM analysis. His primary responsibility at the CFN is to provide support and training for the scientific staff that use the high-resolution electron microscope facility at the



**George Wei** is a research staff engineer and member of the Energy Conversion Group at Brookhaven National Laboratory. He earned his mechanical engineering degree in China and has many years of experience at BNL working on designing and building energy systems and performing combustion related research.



**Yusuf Celebi** is a chemical engineer working with the Energy Conversion Group at Brookhaven National Laboratory. He earned his master and bachelor degrees in chemical engineering from the City College of New York. Over the years he worked on many different projects that include residential heating system efficiency and emission, hydrogen storage, high nickel content lithium-ion battery cathode materials, and geothermal materials research.